ERJ Express. Published on May 31, 2018 as doi: 10.1183/13993003.00457-2018

EUROPEAN RESPIRATORY *journal*

FLAGSHIP SCIENTIFIC JOURNAL OF ERS

Early View

Original article

The mucin bundles responsible for airway cleaning are retained in cystic fibrosis and by cholinergic stimulation

Anna Ermund, Lauren N. Meiss, Brendan Dolan, Andrea Bähr, Nikolai Klymiuk, Gunnar C. Hansson

Please cite this article as: Ermund A, Meiss LN, Dolan B, *et al*. The mucin bundles responsible for airway cleaning are retained in cystic fibrosis and by cholinergic stimulation. *Eur Respir J* 2018; in press (https://doi.org/10.1183/13993003.00457-2018).

The mucin bundles responsible for airway cleaning are retained in cystic fibrosis and by cholinergic stimulation

Anna Ermund[1], Lauren N. Meiss[1], Brendan Dolan[1], Andrea Bähr[2], Nikolai Klymiuk[2] and Gunnar C. Hansson[1,*]

Affiliations [1]Department of Medical Biochemistry, University of Gothenburg, Sweden; [2]Institute of Molecular Animal Breeding and Biotechnology, Gene Center, Ludwig-Maximilians-University Munich, Germany.

Correspondence: Gunnar C. Hansson, Department of Medical Biochemistry, University of Gothenburg, Box 440, SE-405 30 Gothenburg, Sweden. E-mail: gunnar.hansson@medkem.gu.se

Take home message: Acetylcholine uncouples airway surface liquid transport from transport of the mucus bundles and lack of CFTR inhibits bundle movement.

ABSTRACT

The beneficial effect of anti-cholinergic therapy for chronic obstructive pulmonary diseases like COPD is well-documented although cholinergic stimulation paradoxically inhibits liquid absorption, increases cilia beat frequency, and increases airway surface liquid transport.

Using pig tracheobronchial explants, we quantified basal mucus transport as well as after incubation with by the clinically used anti-muscarinic compound ipratropium bromide (Atrovent) and stimulation with acetylcholine.

As expected the surface liquid transport was increased by acetylcholine and carbachol. In contrast, the mucus bundles secreted from the submucosal glands normally transported on the cilia were stopped from moving by acetylcholine, an effect inhibited by ipratropium bromide. Interestingly, in pigs lacking a functional CFTR channel, the mucin bundles were almost immobile. As in wild-type pigs the cystic fibrosis (CF) surface liquid transport increased after carbachol stimulation. The stagnant CF mucin bundles were trapped on the tracheal surface attached to the surface goblet cells. *Pseudomonas aeruginosa* bacteria were moved by the mucus bundles in wild-type, but not CF pigs.

Acetylcholine thus uncouples airway surface liquid transport from transport of the surface mucin bundles as the bundles are dynamically inhibited by acetylcholine and the CFTR channel, explaining initiation of CF and COPD and opening novel therapeutic windows.

Introduction

Airway mucus obstruction is common to many chronic lung diseases such as asthma, chronic obstructive pulmonary disease (COPD) as well as cystic fibrosis (CF) and contributes substantially to airflow limitations [1]. This is caused by increased vagal tone and increased levels of acetylcholine (ACh) that causes increased airway smooth muscle tone. In addition ACh also causes submucosal gland secretion, increased ciliary beat frequency and inhibits air surface liquid absorption [2, 3]. Treating airway diseases with muscarinic antagonists to block parasympathetic signaling is an old tradition, but it was not until the introduction of non-absorbable atropine derivatives as ipratropium became an accepted therapy used especially for COPD. However, the beneficial effect of anti-cholinergic treatment, except for the muscle-relaxing effect, is paradoxically partly opposite to what could be considered physiologically beneficial.

The respiratory tract is kept essentially free from inhaled particles and bacteria by the mucociliary clearance system. The constantly beating cilia generate an escalator transporting mucus cephalically to the larynx. As the organization of the mucus system differs between the commonly used small experimental animals and higher species there has been some confusion. Mice essentially lack submucosal glands, whereas humans and pigs have numerous glands [2]. Submucosal glands produce the MUC5B mucin that forms linear polymers [4]. In the submucosal glands, the most peripheral cells generate a chloride- and bicarbonate-rich fluid that passes by the MUCB secreting cells and by this unfolds and pulls out the MUC5B polymers [5, 6]. During the duct passage these polymers form thick mucin bundles that are 25-30 μm thick and made up of >1,000 polymers. The bundles appear from the gland openings and are then moving in or on top of the 7-10 μm deep airway surface liquid (ASL) with a mean velocity of 0.3 μm/min [2, 6]. The

ASL moves faster (3-5 μm/min) than the bundles, a discrepancy we suggest to be caused by the mucus bundles being anchored to the surface goblet cells [6]. We have now studied the mucus bundle transport on live tracheal tissue from normal newborn piglets and piglets lacking the CFTR channel as in cystic fibrosis (CF) and can show that ACh blocks the mucus bundle movement and thus we give additional explanation for the beneficial effect of ipratropium bromide (Atrovent) whereas in CF the mucus bundles were essentially immobile.

Material and methods

Piglets and airway preparation.

All animal procedures were performed according to the German Animal Welfare Act with permission of the local regulatory authority. Breeding of CF and WT littermate piglets was performed as described [7]. Births were induced and airways dissected and shipped as described [6] within 24 hours of birth. For further methods see Supplemental material.

Statistical analysis.

All statistical tests were performed using GraphPad Prism 7.02 and all data are represented as mean ± standard error of the mean (SEM). Each time-lapse was considered as one replicate. Differences were assessed with two-tailed Mann-Whitney U-test to compare two groups and Kruskal-Wallis test followed by Dunn´s multiple comparisons test were employed for multiple comparisons as appropriate and $P < 0.05$ was defined as significant. No statistical methods were used to predetermine sample size and no randomization was employed. No animals were excluded from the analyses and because the morphology of CF piglet trachea is distinct, the experiments could not be performed blinded to the observer.

Results

Cholinergic inhibition by Ipratropium bromide promotes mucus bundle transport.

Mucus bundles from submucosal glands clean the airways by sweeping over the surface to collect debris and bacteria [6]. The movement of these Alcian blue stained mucus bundles can be studied in explant piglet airways mounted in a temperature controlled chamber [6]. The uneven movement of the Alcian blue stained mucus bundles is best illustrated by movies (Movie S1). Cholinergic signaling has been claimed to be increased in lung diseases such as COPD [8], asthma [9], and CF [10]. To mimic this situation we added the metabolically more stable acetylcholine (ACh) analog carbachol (Cch) to the chamber and studied the mucus bundle transport in WT piglet trachea. Surprisingly, the transport of mucus bundles was essentially stopped by Cch (figure 1a). To exclude off-target effects, we next tested the endogenous transmitter acetylcholine (ACh) on the transport of Alcian blue stained mucus bundles and found that ACh exerted the same effect as Cch. The ACh stopped mucus was mobilized again by the non-selective muscarinic receptor antagonist ipratropium bromide. Interestingly, the ipratropium bromide effect lasted only 45 min as the transport was back to the ACh levels 45 min after ipratropium removal (figure 1b). Ipratropium bromide did not inhibit the formation of Alcian blue stained bundles either before (figure 1c) or after ACh stimulation (figure 1d).

Mucociliary transport, often referred to as mucus transport, is traditionally visualized by the movement of particles on the mucosal surface [11]. Similar to others [12], we used 40 nm carboxylated fluorescent beads added to piglet airway preparations. As shown previously [6], Alcian blue and beads stained distinct material in WT (figure S1, Movie S2).

The Alcian blue bundles exited the submucosal gland openings (figure 2a, green arrow) and the carboxylated beads gathered in dots on the epithelial surface and sometimes in linear patterns (figure 2a). The Alcian blue bundles and beads did not stain the same shapes (figure S2). To further address the differences, the velocity of the beads and bundles were compared showing that the beads moved with higher velocity than the Alcian blue stained bundles (figure 2b). Furthermore, adding Cch caused the beads to move even faster at the same time as the Alcian blue stained mucus bundles further slowed down within 5 min of Cch application (figure 2b). The fluorescent beads thus responded to ACh stimulation by an increased transport as previously observed for mucociliary clearance of what has been called mucus and corresponds to the airway surface liquid (ASL). To avoid confusion, we suggest using ASL for the liquid directly transported by the cilia. The bead-gathering strands are in the ASL and their velocity given as ASL.

Immunostaining for the MUC5AC and MUC5B mucins illustrated that the main mucin in the glands is MUC5B whereas the surface goblet cells contain mainly MUC5AC (figure 2c). Mucus bundles exiting submucosal glands was previously identified in WT piglet airways with scanning electron microscopy (SEM) [6] and as humans also have numerous submucosal glands, we found the same type of mucus bundles on the human airway surface (figure 2d).

Mucus bundles are immobile in CF trachea.

Cystic fibrosis (CF) is a disease caused by a non-functional CFTR and characterized by decreased mucociliary clearance and mucus accumulation. When the transport velocity of Alcian blue stained mucus bundles in neonatal WT and CF piglet tracheas was compared, a dramatic impairment in mucus transport was observed in CF airways (figure 3a). Time-lapse recordings of Alcian blue stained CF tracheas revealed a very slow transport (Movie S3). To study whether

ipratropium bromide could abrogate the decreased velocity in CF, similar to what was observed in WT, we measured Alcian blue stained bundle velocity after ipratropium bromide treatment. Preincubation with ipratropium had no direct effect in CF (figure 3b). Addition of ACh further arrested the bundle movement in CF and preincubation with ipratropium had no rescuing effect. A similar pattern of bundles was noted on CF as WT trachea after ipratropium (figure 3c) but ACh stimulation did not cause additional mucus secretion, in contrast to WT trachea (figure 3d).

Scanning electron micrographs of CF tracheas showed long bundles exiting submucosal glands (figure 4a, green arrow), immunostaining MUC5B in submucosal glands, and MUC5AC in surface goblet cells (figure 4b), similar to WT. As in WT tracheas, we studied the transport of fluorescent beads and Alcian blue stained mucus bundles. The beads collected in similar shapes as in WT and moved toward the larynx (Movie S4). When the images were superimposed, it was clear that the beads did not overlap with the Alcian blue staining (Movie S5). Just as in WT, there was a tendency for the beads to move faster after Cch stimulation, whereas the movement of Alcian blue stained bundles slowed down (figure 4c,d). Thus the ASL and mucus bundles had opposite responses also in CF, although the velocities were considerably lower.

MUC5B mucus bundles from submucosal glands are retained by MUC5AC from surface goblet cells in CF

The Alcian blue stained bundles had a core of MUC5B stained with the *Lotus tetragonolobus* lectin (LTL) [6] in both WT and CF (figure 5a,c). Live WT piglet trachea mucus bundles stained with fluorescein-labeled LTL, but the fluorescent beads did not bind to the LTL-positive mucus bundles as they appeared directly from the submucosal glands (figure 5b, d). Thus, the bundles exited the gland without binding beads, but at later time points the mucus bundles collected beads, suggesting that the material that collected the beads later also gathered on the bundles.

Thus the mucus bundles stained with Alcian blue or LTL were distinct from the fluorescent beads, similar to WT.

The thickness of the Alcian blue stained bundles was similar in WT and CF (figure 6a). The bundle thickness estimated from LTL-staining was also similar with a tendency for thinner in CF (figure 6b). It has been suggested that the mucus bundles were trapped in the glands of CF [12], a phenomenon that might give less mucus bundles in CF. When the total volume of lectin stained bundles was measured, no major differences were observed (figure 6c).

We have previously demonstrated that bicarbonate in sufficient amounts is necessary for a normal detachment of the mucus in the small intestine and that removal of serosal bicarbonate caused WT intestine to mimic CF [13]. When bicarbonate was removed from the buffer on WT tracheal explants stained with Alcian blue, the transport was as slow as in CF (figure 6d), emphasizing the importance for bicarbonate and functional CFTR.

Mucus bundles are retained by MUC5AC from surface goblet cells in CF.

To explore how the bundle transport was slowed in CF, we stained the MUC5B bundles with LTL (green) and the MUC5AC mucin from the surface goblet cells with the UEA1 lectin (red) (figure 2c, 4b). In WT (figure 7a) and in CF (figure 7c), the bundles consisted of a core of MUC5B coated with MUC5AC [6]. The contact points between the bundles and the goblet cells could be observed in confocal images at higher magnification (figure 7a´, 7c') and in SEM images (figure 7b, 7d). In both WT and CF the MUC5AC mucin appeared from the tracheal surface goblet cells, coated the MUC5B bundles and connected the two. The distance between the bundles and the epithelium were measured, revealing a tendency for a shorter distance in CF compared to WT (figure 8a). Interestingly, the number of contact points between goblet cells and bundles assessed as MUC5AC stained connections was significantly higher in CF (figure 8b).

To illustrate the consequences of the observed differences in mucus bundle movement for cleaning the tracheal surface from bacteria, we added TAMRA-stained *Pseudomonas aeruginosa* bacteria (red) to LTL-stained bundles (green) on piglet trachea (figure 8cd). In the WT animals the bacteria were quickly collected on the moving bundles and leaving the surface essentially free of bacteria (figure 8c, Movie S6). In contrast, the bacteria covered the surface of the epithelium in CF and the bacteria on the bundles were essentially stagnant (figure 8d, Movie S7). The mucus bundles sweeping over the tracheal surface are thus essential for cleaning the tracheobronchial surface and the stagnant bundles in CF result in inefficient clearing of bacteria from the epithelial surface.

Discussion

Analyzing mucus *in vivo* or *ex vivo* in a physiological way is challenging. A major problem is that mucus is completely transparent and thus invisible. The cationic Alcian blue dye binds to the multiple negative charges found on the glycans of the mucin domains and has been used for decades to stain mucus on tissue sections. We have now taken advantage of this and used Alcian blue to stain live tracheobronchial explants. To our initial surprise, we observed thick Alcian blue stained mucus bundles appearing from submucosal glands openings [6]. Other scientists have used 40 nm fluorescent beads to stain ‘mucus’ [14]. These beads are carboxylate-modified and thus negatively charged. These beads did not bind the mucus bundles, but gathered on other structures of unknown identity very weakly stained by Alcian blue or LTL. The Alcian blue bundle and bead transport were affected in opposite directions by Cch stimulation in both WT and CF. This further supports that Alcian blue and fluorescent beads label distinct materials. The increased transport velocity of the beads after Cch is similar to what has been observed for

mucociliary clearance using for example micro-OCT [2, 15]. This surface liquid has often been called ‘mucus’, but in the normal lung this is the same as the airway surface liquid (ASL). To avoid confusion, we use the name ASL for the bead transport. This normal ASL should be kept separate from the mucus that accumulates at the epithelial surface upon disease observed on human bronchial epithelial cultures [16].

Lungs in pigs and humans have numerous submucosal glands ideally organized to make mucus bundles from linear MUC5B mucin polymers [5]. In the normal lung, these mucus bundles are transported cephalically and by this sweeping the tracheal surface [6]. The normal tracheobronchial surface is covered by ASL of about 10 µm, of which 4-5 µm is occupied by cilia in pigs and humans [2]. The mucus bundles are substantially thicker (average thickness 27 µm) than the ASL depth and thus the bundles are moving on top of and partly dipping into the ASL.

During the transport cephalically the mucus bundles from the glands were covered with material from surface goblet cells both in WT and CF. This material contained the MUC5AC mucin, was stained by the UEA1-lectin, and connected the surface goblet cells with the bundles. The distance between the bundles and epithelial surface was similar in WT and CF, but the number of connections were four times higher in CF. As bundles appeared from both WT and CF glands and were found on the tracheal surface to about the same extent, we find it difficult to envision that the mucus bundles were attach specifically to the gland openings, as has been suggested elsewhere [12, 17]. In contrast, our results suggest that the mucus bundles were anchored to the surface goblet cells in CF. The observations that the MUC5B core of the mucus bundles is coated with the MUC5AC mucin and that goblet cells are found also in the gland ducts [2, 6] provide an explanation to how the mucus bundles can be observed to be retained in gland openings in CF. Our results suggest that the surface mucus bundles are anchored to the epithelial

surface goblet cells and that the bundles are kept at the surface and thereby hindered from falling out into the tracheal lumen. As the mucus bundles are transported up to ten times slower than the ASL, we further hypothesize that the bundle transport is controlled by attachment-detachment of the goblet cell-bundle anchors. This is similar to what we observed in the small intestine, where a specific protease is required for detaching the mucins from the goblet cell anchor [13, 18].

CF is characterized by stagnant mucus that permits bacterial overgrowth. We now show that the mucus bundles were essentially stationary in the newborn CF piglets as well as in WT when bicarbonate was removed. Since the piglets were less than 24 h old at analysis, our results suggest that also human CF lung disease starts already at birth, strongly suggesting that treatment of human CF should start early.

In addition, *Pseudomonas aeruginosa* bacteria added to the tracheas were rapidly removed from the WT, but not CF tissues. This can be observed as higher background in the CF images. If the cause of this difference is more or less specific binding to the epithelial surface or the absence of the bundle sweeping, or a combination of these is not known. The important point is that in CF there is already from birth a defect in airway cleaning and the bacterial accumulation can be assumed to cause lung disease.

The cholinergic system is important for respiratory physiology as the vagus nerve uses ACh to increase airway smooth muscle tone, submucosal gland secretion, and ciliary beat frequency at the same time as it inhibits surface liquid absorption [2, 3]. Increased cholinergic tonus is common in asthma and COPD [8, 9] and the muscarinic inhibitor ipratropium bromide (Atrovent®) is used for pharmacological treatment of COPD. The use of this treatment is rather counterintuitive except for its inhibitory effect on bronchoconstriction. However, the quick effect of ACh discovered stopped the transport of mucus bundles and suggests another novel mechanism that could explain some of the beneficial effect of anti-cholinergic treatment.

Ipratropium with its anti-muscarinic M_1, M_2, and M_3 receptor inhibition, efficiently reversed this effect. Newborn normal piglet tracheas do of course not represent the lung phenotype of a patient with COPD as these patients have accumulated mucus and plugged airways. Still COPD patients have a clinically documented beneficial effect of ipratropium bromide and we suggest that this is due to its anti-cholinergic effect counteracting ACh induced reduced mucus bundle transport. In COPD patients, this effect might be localized to less affected parts. Clinical outcomes of ipratropium bromide in COPD are presented elsewhere [19]. Ipratropium bromide had little effect in newborn CF piglets indicating that initial CF disease is acting by a different mechanism than in COPD. However, the lack of effect in initial CF disease does not mean lack of effect in advanced CF disease [20].

Increased vagal tone and ACh is the physiological response to dust inhalation and the effect to block bundle movement while the ASL is simultaneously moving faster is a logical one to more efficiently collect the debris onto the mucus bundles before these are detached and capable of efficiently transporting the debris to the larynx. Our results further suggest that mucus bundle movement is controlled by attachment-detachment of the mucus bundles to the surface goblet cells.

Financial support

This work was supported by the European Research Council, Swedish Research Council, The Swedish Cancer Foundation, The Knut and Alice Wallenberg Foundation, IngaBritt and Arne Lundberg Foundation, Sahlgrenska University Hospital (ALF), Wilhelm and Martina Lundgren's Foundation, National Institute of Allergy and Infectious Diseases (U01AI095473), Erica Lederhausen's Foundation, The Swedish Heart-Lung Foundation, the Swedish Cystic Fibrosis

Foundation, Magnus Bergvall´s Foundation, Lederhausen's Center for CF Research at Univ. Gothenburg, and the Cystic Fibrosis Foundation (CFFT, Hansso14X0).

Acknowledgements

We are indebted to Drs. Jeffery Wine, Stanford University and David Thornton, University of Manchester for valuable discussions.

References

1. Gosens R, Zaagsma J, Meurs H, Halayko AJ. Muscarinic receptor signaling in the pathophysiology of asthma and COPD. *Respir Res* 2006; 7: 73.
2. Widdicombe JH, Wine JJ. Airway Gland Structure and Function. *Physiol Rev* 2015; 95: 1241-1319.
3. Buels KS, Fryer AD. Muscarinic Receptor Antagonists: Effects on Pulmonary Function. *Handbook of Experimental Pharmacology,* 2012; 208: 317-341.
4. Ridley C, Kouvatsos N, Raynal BD, Howard M, Collins RF, Desseyn JL, Jowitt TA, Baldock C, Davis CW, Hardingham TE, Thornton DJ. Assembly of the Respiratory Mucin MUC5B: a new model for gel-forming mucin. *J Biol Chem* 2014; 289: 16409-16420.
5. Trillo-Muyo S, Nilsson HE, Recktenwald CV, Ermund A, Ridley C, Meiss LN, Bahr A, Klymiuk N, Wine JJ, Koeck PJ, Thornton DJ, Hebert H, Hansson GC. Granule-stored MUC5B mucins are packed by the non-covalent formation of N-terminal head-to-head tetramers. *J Biol Chem* 2018; 293: 5746-5754.
6. Ermund A, Meiss LN, Rodriguez-Pineiro AM, Bähr A, Nilsson HE, Trillo-Muyo S, Ridley C, Thornton DJ, Wine JJ, Hebert H, Klymiuk N, Hansson GC. The normal trachea is cleaned by MUC5B mucin bundles from the submucosal glands coated with the MUC5AC mucin. *Biochem Biophys Res Commun* 2017; 492: 331-337.
7. Klymiuk N, Mundhenk L, Kraehe K, Wuensch A, Plog S, Emrich D, Langenmayer MC, Stehr M, Holzinger A, Kroner C, Richter A, Kessler B, Kurome M, Eddicks M, Nagashima H, Heinritzi K, Gruber AD, Wolf E. Sequential targeting of CFTR by BAC vectors generates a novel pig model of cystic fibrosis. *J Mol Med (Berl)* 2012; 90: 597-608.
8. Gross NJ, Co E, Skorodin MS. Cholinergic bronchomotor tone in COPD. Estimates of its amount in comparison with that in normal subjects. *Chest* 1989; 96: 984-987.
9. Ayala LE, Ahmed T. Is there loss of protective muscarinic receptor mechanism in asthma? *Chest* 1989; 96: 1285-1291.
10. Larsen GL, Barron RJ, Cotton EK, Brooks JG. A comparative study of inhaled atropine sulfate and isoproterenol hydrochloride in cystic fibrosis. *Am Rev Respir Dis* 1979; 119: 399-407.
11. Wanner A. Clinical aspects of mucociliary transport. *Am Rev Respir Dis* 1977; 116: 73-125.
12. Hoegger MJ, Fischer AJ, McMenimen JD, Ostedgaard LS, Tucker AJ, Awadalla MA, Moninger TO, Michalski AS, Hoffman EA, Zabner J, Stoltz DA, Welsh MJ. Impaired mucus detachment disrupts mucociliary transport in a piglet model of cystic fibrosis. *Science* 2014; 345: 818-822.
13. Gustafsson JK, Ermund A, Ambort D, Johansson MEV, Nilsson HE, Thorell K, Hebert H, Sjovall H, Hansson GC. Bicarbonate and functional CFTR channel is required for proper mucin secretion and link Cystic Fibrosis with its mucus phenotype. *J Exp Med* 2012; 209: 1263-1272.
14. Hoegger MJ, Awadalla M, Namati E, Itani OA, Fischer AJ, Tucker AJ, Adam RJ, McLennan G, Hoffman EA, Stoltz DA, Welsh MJ. Assessing mucociliary transport of single particles in vivo shows variable speed and preference for the ventral trachea in newborn pigs. *Proc Natl Acad Sci USA* 2014; 111: 2355-2360.

15. Birket SE, Chu KK, Liu L, Houser GH, Diephuis BJ, Wilsterman EJ, Dierksen G, Mazur M, Shastry S, Li Y, Watson JD, Smith AT, Schuster BS, Hanes J, Grizzle WE, Sorscher EJ, Tearney GJ, Rowe SM. A Functional Anatomic Defect of the Cystic Fibrosis Airway. *Am J Resp Critical Care Med* 2014; 190: 421-432.
16. Matsui H, Grubb BR, Tarran R, Randell SH, Gatzy JT, Davis CW, Boucher RC. Evidence for periciliary liquid layer depletion, not abnormal ion composition, in the pathogenesis of cystic fibrosis airways disease. *Cell* 1998; 95: 1005-1015.
17. Ostedgaard LS, Moninger TO, McMenimen JD, Sawin NM, Parker CP, Thornell IM, Powers LS, Gansemer ND, Bouzek DC, Cook DP, Meyerholz DK, Abou Alaiwa MH, Stoltz DA, Welsh MJ. Gel-forming mucins form distinct morphologic structures in airways. *Proc Natl Acad Sci USA* 2017; 114: 6842-6847.
18. Schütte A, Ermund A, Becker-Pauly C, Johansson MEV, Rodriguez-Pineiro AM, Bäckhed F, Müller S, Lottaz D, Bond JS, Hansson GC. Microbial Induced Meprin beta Cleavage in MUC2 Mucin and Functional CFTR Channel are Required to Release Anchored Small Intestinal Mucus. *Proc Natl Acad Sci USA* 2014; 111: 12396-12401.
19. Li X, Obeidat M, Zhou G, Leung JM, Tashkin D, Wise R, Connett J, Joubert P, Boss+® Y, van den Berge M, Brandsma CA, Nickle DC, Hao K, Par+® PD, Sin DD. Responsiveness to Ipratropium Bromide in Male and Female Patients with Mild to Moderate Chronic Obstructive Pulmonary Disease. *EBioMedicine* 2017; 19: 139-145.
20. Bradley JM, Koker P, Deng Q, Moroni-Zentgraf P, Ratjen F, Geller DE, Elborn JS. Testing two different doses of tiotropium Respimat(R) in cystic fibrosis: phase 2 randomized trial results. *PLoS ONE* 2014; 9: e106195.

Figure legends

FIGURE 1 Cholinergic inhibition promotes mucus transport. a) Alcian blue stained mucus bundles essentially stopped moving after carbachol (Cch) stimulation, n = 45 wild type (WT) control and 12 Cch time lapses, p = 0.0001. b) Ipratropium bromide reversed the decreased movement induced by acetylcholine (ACh), n = 7 Ipratropium, 5 Ipratropium + Cch <45 min, 9 Ipratropium + Cch >45 min, 8 ACh time lapses, p = 0.03. c) Live submerged WT piglet trachea preincubated with 100 nM ipratropium bromide for 1 hour and stained with Alcian blue. d) WT piglet trachea incubated with ipratropium bromide after stimulation with ACh. Scale bar in c and d, 1 mm. Data analyzed by two-tailed Mann-Whitney U-test.

FIGURE 2 Submucosal glands secrete mucus bundles stained by Alcian blue. a) Alcian blue stained bundle (blue) from submucosal gland and beads (orange). Arrow points to gland opening. b) Velocity of bead-collecting strands (open bars, ASL) and Alcian blue stained bundles (black bars, bundles) without or with 100 μM Carbachol (Cch). The beads moved faster than Alcian blue stained bundles in both cases, n = 41 Alcian blue, 9 beads, 7 Alcian blue with Cch, 9 beads with Cch time lapses, p = 0.03 for no Cch and p = 0.0003 for 100 μM Cch. Data analyzed by two-tailed Mann-Whitney U-test. c) The MUC5B mucin (green) was expressed mainly in the submucosal glands and to a minor extent in the surface goblet cells whereas the MUC5AC mucin (red) was expressed exclusively in the airway surface goblet cells in WT piglet trachea. d) Bundle on the cilia observed with scanning electron microscopy (SEM) in human trachea. Experiments in a and c were performed on at least 4 pigs. Scale bar in a 250 μm, c 50 μm and d 2 μm.

FIGURE 3 Mucus bundles are immobile in CF piglet tracheas. a) Comparison of transport velocity for Alcian blue stained bundles in WT and CF piglet trachea, n = 39 WT and 32 CF, p = 0.03. b) In CF, ACh stimulation decreased transport velocity of Alcian blue stained bundles, even after preincubation with Ipratropium bromide, n = 18 CF control, 7 Ipratropium, 7 Ipratropium + ACh <45 min, 7 ACh time lapses, p = 0.0003 CF control compared to ACh, p = 0.0034 CF control vs. Ipratropium + ACh <45 min, no difference between Ipratropium + ACh <45 min and ACh alone and no difference between control and ipratropium alone, Kruskal-Wallis multiple comparisons test with Dunn´s post hoc test. c) CF piglet trachea stained with Alcian blue after preincubation with 100 nM ipratropium bromide for 1 hour. d) CF trachea incubated with ipratropium bromide, stained with Alcian blue and stimulated with ACh. Scale bar in c and d 1 mm.

FIGURE 4 Submucosal glands in CF piglets secrete Alcian blue stained mucus bundles. a) Bundles formed in CF piglet trachea visualized by SEM, submucosal gland opening indicated by green arrow. b) Similar expression pattern in CF piglet trachea as in WT. Experiments in a and b were performed on at least 4 pigs. Scale bar in a 50 μm, in b 25 μm. c) Velocity of bead-collecting strands (white bars, ASL) and Alcian blue stained bundles (black bars, bundles) without or with 100 μM Cch. The beads moved faster than Alcian blue stained bundles. The beads moved faster than Alcian blue stained bundles when stimulated with 100 μM Cch, p = 0.03. d) Focus on the Alcian blue bundle movement in c, p = 0.043, n = Alcian blue 34, beads 8, Alcian blue 100 μM Cch 9 and beads 100 μM Cch 13 time-lapses. Data analyzed by two-tailed Mann-Whitney U-test. Scale bar in a 50 μm and 25 μm in b.

FIGURE 5 Mucus bundles stained with Alcian blue and LTL-lectin, but not beads. a) Mucus bundles stained with Alcian blue (blue) and LTL (green) in WT piglet trachea. b) Confocal image of a mucus bundle from a WT piglet trachea stained with LTL (green) and with fluorescent beads (magenta). c) Mucus bundles stained with Alcian blue (blue) and LTL (green) in CF piglet trachea. d) Confocal image of a mucus bundle from a CF piglet trachea stained with LTL (green) and with fluorescent beads (magenta). Note large overlap in staining with Alcian blue and the lectin in a and c whereas the beads do not collect on LTL-stained bundles in b and d. Gland opening indicated by dashed line in b and d. Experiment repeated in at least 3 pigs. Scale bar in a and c 1 mm, in c and d 20 μm.

FIGURE 6 Mucus bundle thickness and amount are similar in WT and CF whereas the transport velocity is lower in CF than WT. a) Thickness of Alcian blue stained bundles, WT Alcian n = 8 bundles, n = 3 animals, CF Alcian blue n = 11 bundles, n = 4 animals. b) Thickness of LTL-stained bundles, mean bundle thickness in WT 18 ±4.9 μm, 11 bundles and in CF 12 ±2 μm, 9 bundles, at least 5 measurements per bundle, 3 animals per genotype. c) Mean volume of LTL-stained mucus bundles on an identical surface area of WT and CF trachea (WT, 31 data points; CF, 16 data points from 3 animals each). Results in a, b and c analyzed by two-tailed Mann-Whitney U-test. d) The Alcian blue stained bundles moved with higher velocity on WT than CF trachea, $p = 0.02$ and with higher velocity than WT when bicarbonate was omitted from the buffer, $p = 0.007$, data analyzed by Kruskal-Wallis and Dunn´s multiple comparisons test, n = WT 39, CF 32, WT0bic 36 time-lapses.

FIGURE 7 Mucus bundles are retained by mucus from surface goblet cells in CF. Images from confocal microscopy where the intensities for the lectins is not reflecting relative amounts. a)

Bundles exiting submucosal glands consist of a core of MUC5B (green) and a coating of MUC5AC (red). The coating of MUC5AC comes from surface goblet cells. a´) Detail of a mucus bundle at higher magnification shows how goblet cell mucus reaches out to coat the bundle. b) The contact between mucus bundle and goblet cell was also observed with SEM. c) In CF piglet trachea similar bundles were observed as in WT. c´) Larger magnification showed that the CF bundles had a higher number of contact points than WT bundles. White arrows in a´ and c´ point to attachment points between goblet cell and bundle. d) The contact between bundles and goblet cells in CF was observed with SEM. Scale bar in a 20 μm, a´ 10 μm, b 1 μm, c 20 μm, c´10 μm and in d 1 μm.

FIGURE 8 Model bacterium *Pseudomonas aeruginosa* PAO1 is cleared in WT but not CF trachea. a) Measuring the distance between the epithelium and lectin stained bundles in live tissue revealed a tendency to shorter distance in CF (WT, n = 6 bundles, 5 animals; CF, n = 3 bundles, 3 animals). Data analyzed with two-tailed Mann-Whitney U-test, p = 0.1. b) The number of attachment points were lower in WT than CF (WT, n = 7 bundles, 5 animals; CF, n = 3 bundles, 3 animals). Data analyzed with two-tailed Mann-Whitney U-test, p = 0.008. Representative images are presented in figure 7a and c. c) Mucus bundles stained with LTL (green) and bacteria (red) in WT trachea. d) Mucus bundles stained with LTL (green) and bacteria (red) in CF trachea. Note lack of bacteria on the surface between the bundles in WT. Scale bar in c and d 500 μm.

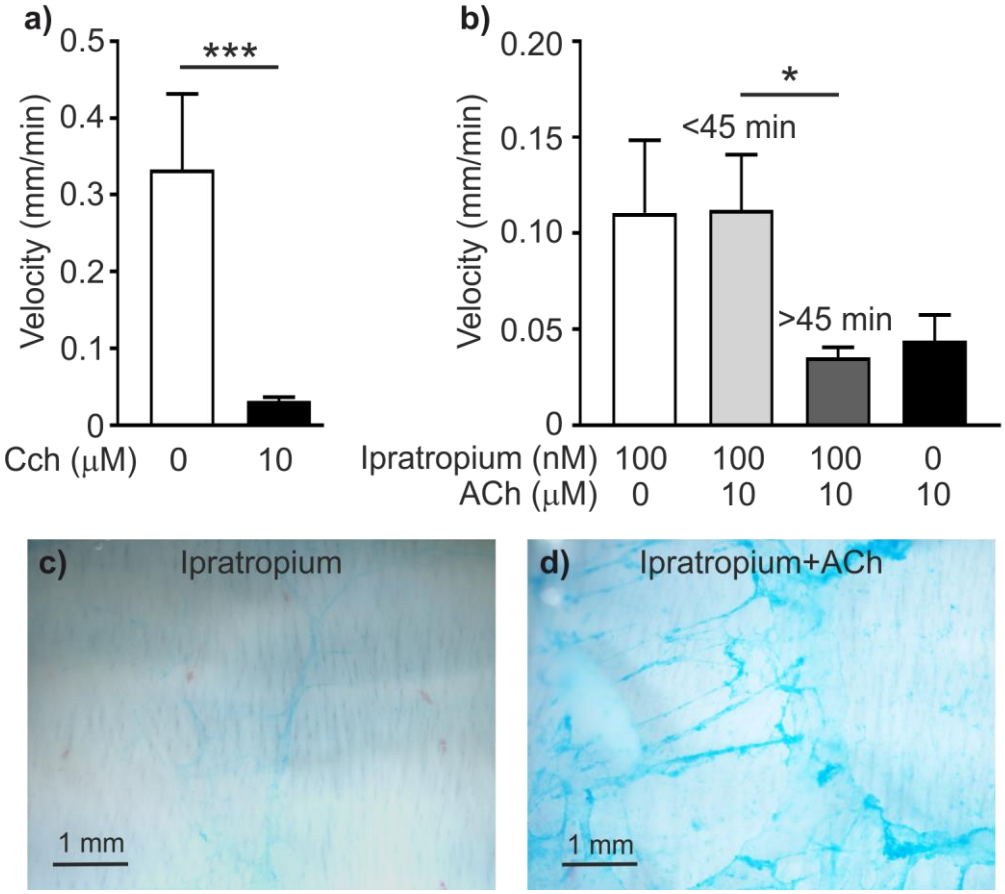
a)
Velocity (mm/min)
0.5
0.4
0.3
0.2
0.1
0
***
Cch (μM) 0 10
b)
Velocity (mm/min)
0.20
0.15
0.10
0.05
0
*
<45 min
>45 min
Ipratropium (nM) 100 100 100 0
ACh (μM) 0 10 10 10
c)
Ipratropium
1 mm
d)
Ipratropium+ACh
1 mm

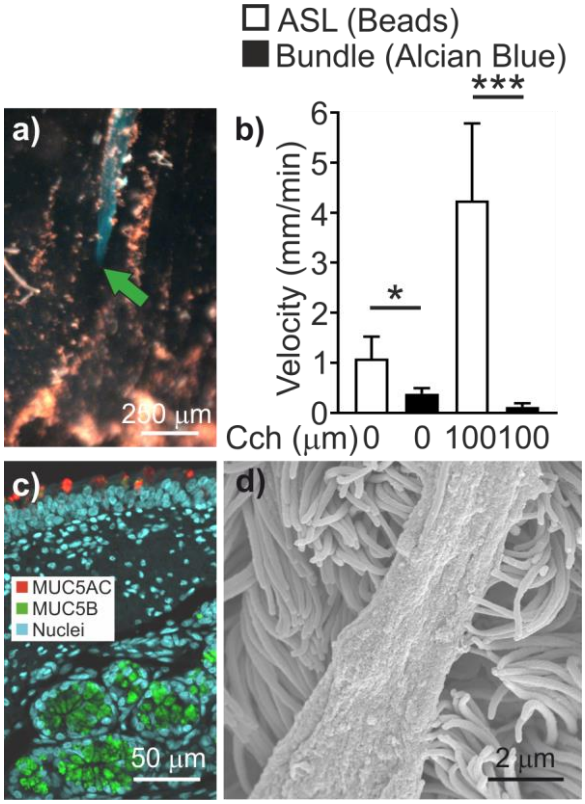
ASL (Beads)
Bundle (Alcian Blue)
a)
200 μm
b)
***
*
Velocity (mm/min)
6
5
4
3
2
1
0
Cch (μm) 0 0 100 100
c)
MUC5AC
MUC5B
Nuclei
50 μm
d)
2 μm

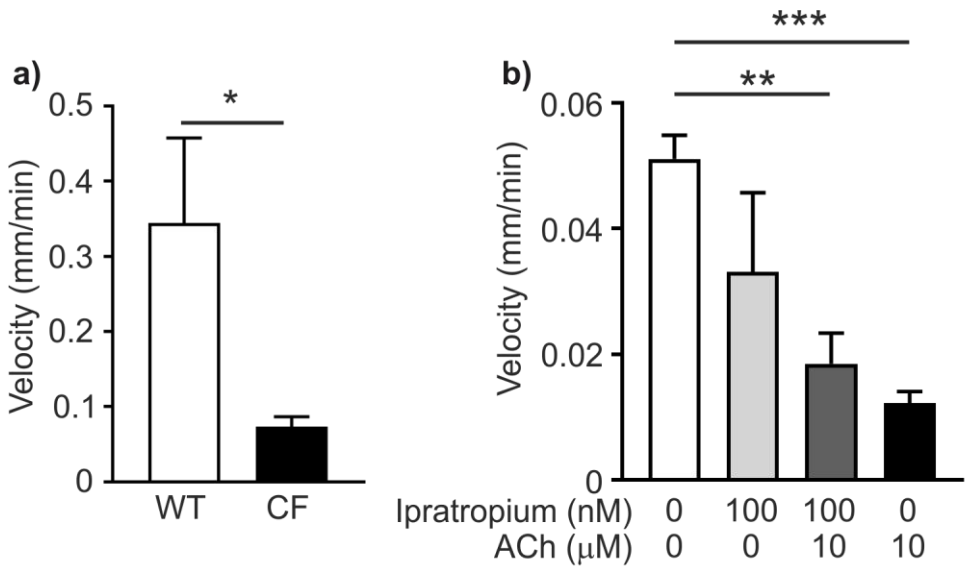
a)
b)
Velocity (mm/min)
0.5
0.4
0.3
0.2
0.1
0
*
WT
CF
***
**
0.06
0.04
0.02
0
Ipratropium (nM) 0 100 100 0
ACh (μM) 0 0 10 10

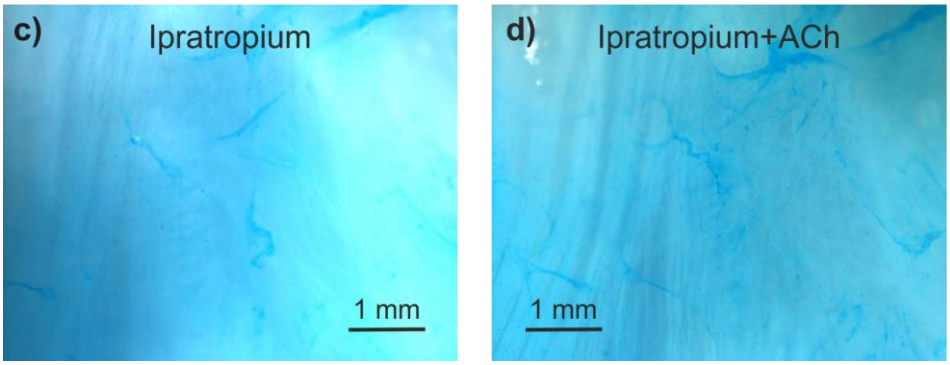
c)
Ipratropium
1 mm
d)
Ipratropium+ACh
1 mm

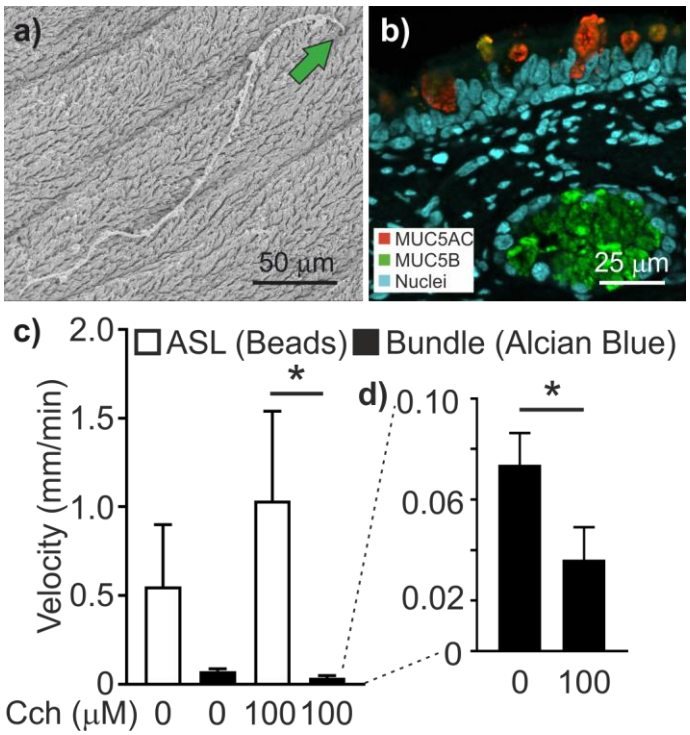
a)
50 μm
b)
MUC5AC
MUC5B
Nuclei
25 μm
c)
ASL (Beads)
Bundle (Alcian Blue)
Velocity (mm/min)
2.0
1.5
1.0
0.5
0
*
d)
0.10
0.06
0.02
0
*
0 100
Cch (μM) 0 0 100 100

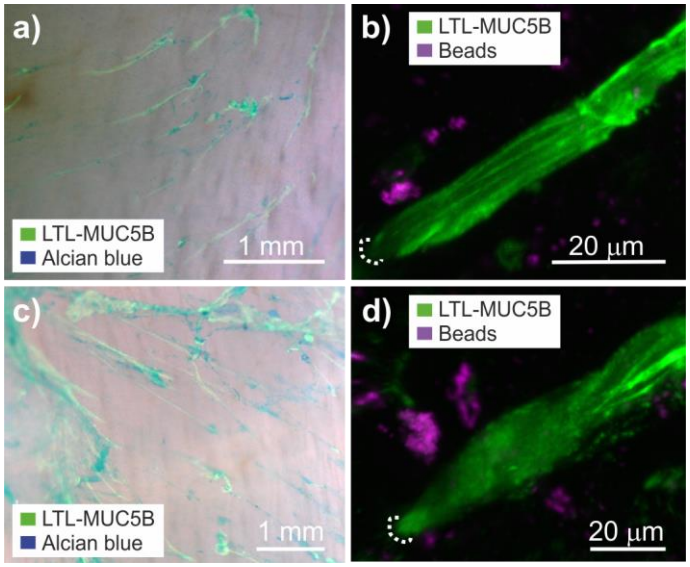
a)
LTL-MUC5B
Alcian blue
1 mm
b)
LTL-MUC5B
Beads
20 µm
c)
LTL-MUC5B
Alcian blue
1 mm
d)
LTL-MUC5B
Beads
20 µm

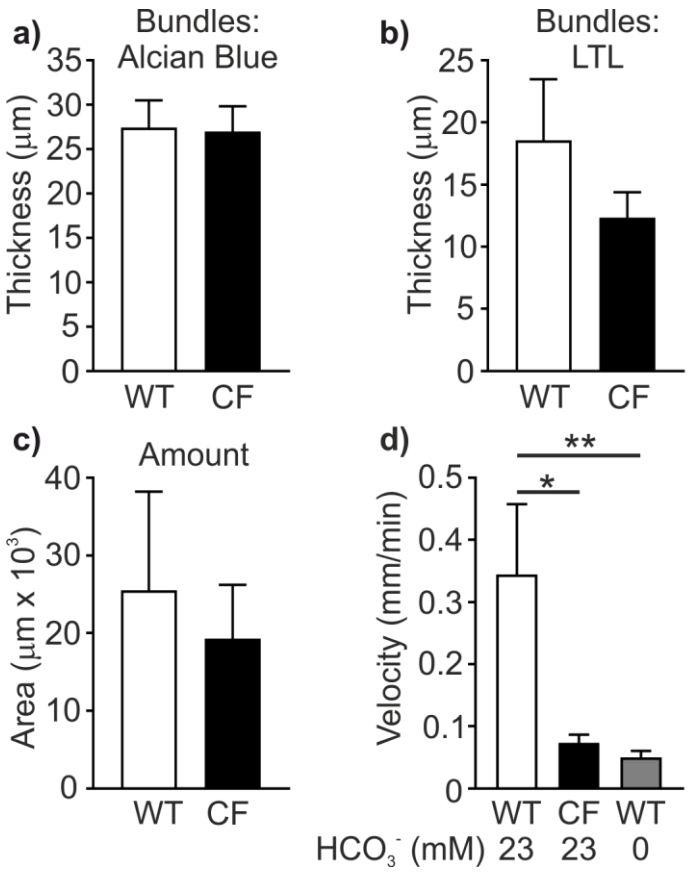
a)
Bundles:
Alcian Blue
Thickness (µm)
35
30
25
20
15
10
5
0
WT
CF
b)
Bundles:
LTL
Thickness (µm)
25
20
15
10
5
0
WT
CF
c)
Amount
Area (µm x 10³)
40
30
20
10
0
WT
CF
d)
**
*
Velocity (mm/min)
0.5
0.4
0.3
0.2
0.1
0
WT
CF
WT
HCO₃⁻ (mM)
23
23
0

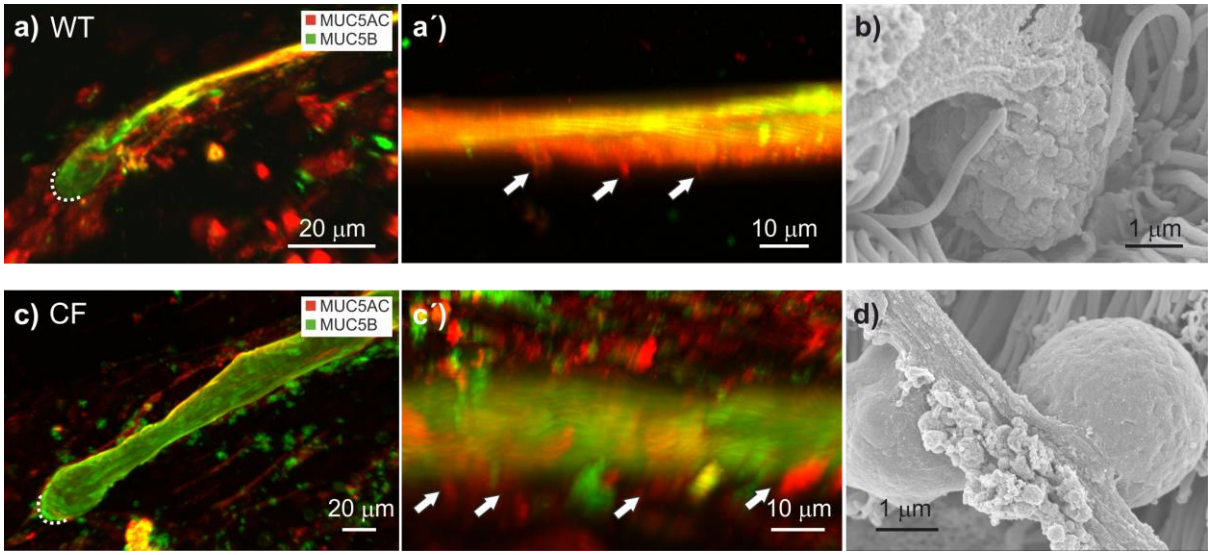
a) WT
MUC5AC
MUC5B
20 µm
a´)
10 µm
b)
1 µm
c) CF
MUC5AC
MUC5B
20 µm
c´)
10 µm
d)
1 µm

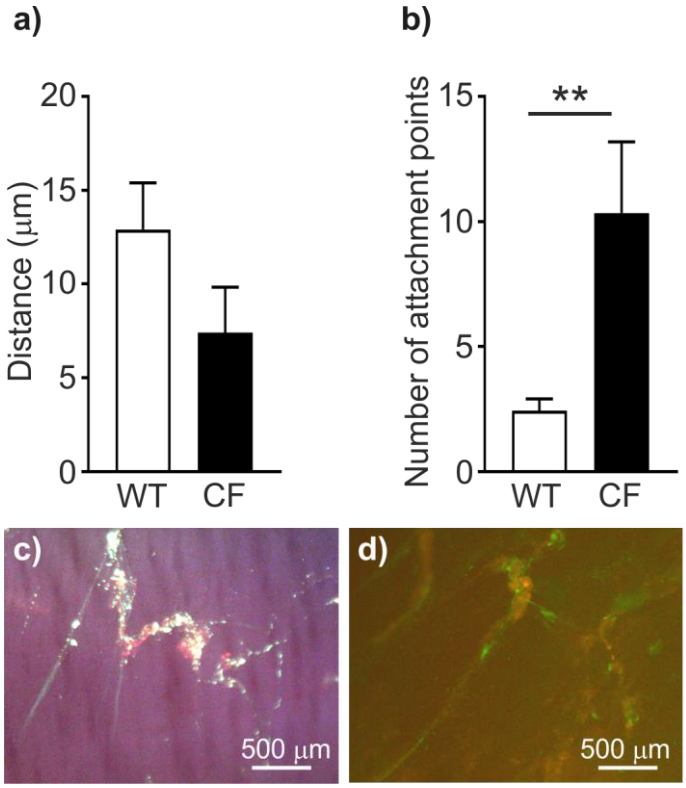
a)
Distance (µm)
20
15
10
5
0
WT
CF
b)
Number of attachment points
15
10
5
0
**
WT
CF
c)
500 µm
d)
500 µm

Supplemental Material

Material and Methods

Video microscopy.

The distal part of neonatal WT and CF pig trachea together with the most proximal part of the primary bronchi were mounted in a Petri dish coated with Sylgard. The tissue was covered in oxygenated (95% O_2, 5% CO_2) Krebs-glucose buffer as described previously {Ermund, 2017 260 /id}. Tissue was heated to 37°C and stained with 0.4 mM Alcian blue 8GX pH 7.4, red (580/605) fluorescent beads (FluoroSpheres™ Carboxylate-modified microspheres, 0.04 μm, ThermoFisher Scientific, Waltham, MA) or fluorescein labeled *Lotus tetragonolobus* lectin (Vector laboratories, Burlingame, CA). Buffer without bicarbonate was prepared by omitting $NaHCO_3$, adjusting the osmolarity with NaCl and adding 10 mM HEPES. Tissue was monitored through a stereo microscope (Nikon, Tokyo, Japan) and white light (Photonics, Pittsfield, MA) or a CoolLED pE-300ultra light source (CoolLED, Andover, UK). Time-lapse recordings were acquired using a 5.0-megapixel color CCD camera (DS-Fi2 or DS-Fi3, Nikon, Tokyo, Japan) or a monochrome cooled-CCD camera (DS-Qi1, Nikon, Tokyo, Japan) and NIS elements software (Nikon, Tokyo, Japan). *Pseudomonas aeruginosa* bacteria were

stained by 6-(Tetramethylrhodamine-5-(and-6)-Carboxamido) Hexanoic Acid, Succinimidyl Ester (TAMRA; ThermoFisher Scientific, Waltham, MA) Bundle transport velocity, Alcian blue bundle thickness and bead-strand thickness were calculated using NIS elements. To calculate transport velocity, the mean of the five fastest-moving points in each time-lapse was taken on moving bundles/strands.

Lectin staining of live tissue for confocal microscopy.

WT and CF pig airway tissue was dissected into 1 cm pieces and opened to expose the luminal surface. Tissue was glued to a Petri dish using Vetbond tissue adhesive (3M, Sollentuna, Sweden) and a mixture of fluorescein labeled *Lotus tetragonolobus* Lectin (LTL), rhodamine labeled *Ulex europaeus* Agglutinin I (UEA1) or FluoroSpheres™ Carboxylate-modified microspheres, 0.04 μm, red fluorescent (580/605) beads (ThermoFisher Scientific, Waltham, MA) were mixed in Krebs-glucose buffer and added to the tissue. After approximately 30 min of incubation at ambient temperature, lectins were removed and fresh Krebs-glucose buffer was added. Tissue was imaged with a Plan-Apochromat ×20/1.0DIC water immersion objective and an upright LSM 700 Axio Examiner 2.1 confocal imaging system (Carl Zeiss, Oberkochen, Germany). Measurements of bundle volume, distance from the epithelium and number of attachment points were performed using the Imaris sorftware (Bitplane, Zurich, Swizerland).

Immunofluorescence staining of fixed sections.

Pig airway tissue was fixed in 4% formalin, embedded in paraffin and cut in 4 μm thick sections, which were dewaxed using Xylene substitute (Sigma, St. Louis, MO) and hydrated in decreasing concentrations of ethanol. Antigen retrieval was performed by microwave heating in 0.01 M citric buffer pH 6. Sections were blocked for 60 min with 3% donkey serum

in Tris-buffered saline (TBS) and permeabilized with 0.1% Triton X-l00. Stainings were performed sequentially. Primary antibodies, mouse monoclonal MUC5AC clone 45M1 (Sigma Aldrich, St. Louis, MO) and MUC5B, kind gift from M. Kesimer (University of South Carolina, Chapel Hill, SC) in blocking solution were incubated over night at 4°C. For MUC5B, donkey anti-rabbit Alexa 488 and for MUC5AC donkey anti-mouse Alexa 647 (Thermo Fisher Scientific, Waltham, MA) secondary antibodies were incubated in blocking solution for two hours at room temperature in the dark. Nuclei were counterstained with Hoechst 34580 (Thermo Fisher Scientific, Waltham, MA). Slides were mounted with Prolong gold mounting medium (Thermo Fisher Scientific, Waltham, MA). Images were acquired with an upright LSM 700 Axio Examiner 2.1 confocal imaging system (Carl Zeiss, Oberkochen, Germany).

Electron microscopy.

WT and CF pig airway tissue was fixed in Karnovsky's fixative (2% paraformaldehyde, 2.5% glutaraldehyde in 0.05 M, sodium cacodylate buffer, pH 7.2) for 24 h at 4°C followed by preparation for scanning electron microscopy (SEM). Postfixation was performed in 1% OsO_4 at 4°C three times with an intervening 1% thiocarbohydrazide step. The samples were dehydrated with increasing concentrations of ethanol followed by hexamethyldisilazane that was allowed to evaporate, samples were mounted on aluminum pins with carbon tabs and finally sputter-coated with palladium before examination at 3 kV in a field emission scanning electron microscope (Zeiss DSM 982 Gemini, Carl Zeiss, Oberkochen, Germany).

Movies:

Movie S1: Alcian blue stained bundles on WT piglet trachea.

Movie S2: Beads gathering on WT piglet trachea.

Movie S3: Alcian blue staining in CF piglet trachea.

Movie S4: Beads on CF piglet trachea.

Movie S5: Alcian blue and beads on CF piglet trachea.

Movie S6: Stained *Pseudomonas aeruginosa* bacteria (red) added to WT piglet trachea with LTL-stained bundles (green).

Movie S7: Stained *Pseudomonas aeruginosa* bacteria (red) added to CF piglet trachea with LTL-stained bundles (green).

All movies collected at 1 frame per second and rendered at 16x original speed.

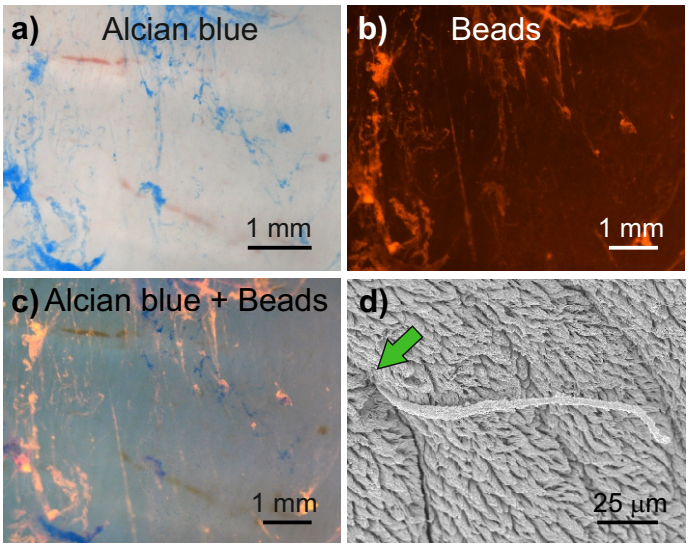

FIGURE S1 Submucosal glands secrete mucus bundles separate from bead-gathering strands in WT piglet trachea. a) WT piglet tracheobronchial preparation stained with Alcian blue. b) WT trachea with fluorescent beads. c) Merge of a and b. d) Bundle exiting the submucosal gland (green arrow) observed with scanning electron microscopy (SEM) in WT piglet trachea. Scale bars in a, b and c 1 mm, in d 25 µm.

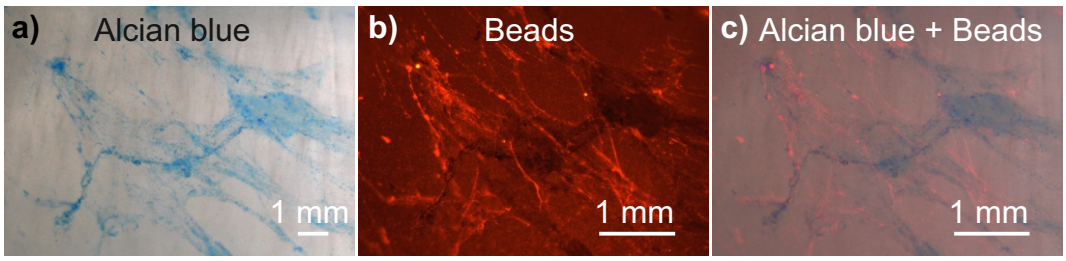

FIGURE S2 Submucosal glands secrete mucus bundles separate from bead-gathering strands in CF piglet trachea. a) CF piglet tracheobronchial preparation stained with Alcian blue. b) CF trachea with fluorescent beads. c) Merge of a and b. Scale bars in a, b and c 1 mm.